Society of Petroleum Engineers
Drilling Systems Automation Technical Section (DSATS)
Drillbotics International University Competition
2015

The University Of Oklahoma
Mewbourne School of Petroleum and
Geological Engineering

Team Members:

Kyle Gustafson[1] (Rig Structure Redesign)

Adaku Akabogu[1] (Circulation System Design)

Zeeneb Alsaihati[1] (Vibration Analysis and Control)

Vimlesh Bavadiya[2] (Bit Sub Design)

Abdulhamid Alsousy[1] (Instrumentation, Measurement and Control Systems)

Faculty Advisor:

Dr. Ramadan Ahmed, Associate Professor

[1] P.E. Undergraduate Student

[2] P.E. Graduate Student

Table of Contents

Figures

Tables

Acknowledgement

We express our gratitude to Dr. Ahmed for his continuous support. We are thankful to him for sharing his vast knowledge and deep insight. We are sincerely grateful for his constructive criticism and advice with issues related to the design improvement. We would also like to expand our deepest gratitude to the University of Oklahoma, Mewbourne School of Petroleum and Geological Engineering for awarding us the opportunity to work on this project.

Executive Summary

The purpose of this project is to provide detailed description of design ideas for a fully automated model drilling rig that can physically simulate a full-scale drilling rig. The University of Oklahoma's Drillbotics team brings to this year's competition a drilling rig design that has been inspired from the knowledge gained from previous year's competition.

Drill rig travelling assembly/structure, circulation system, vibrations analysis and control, bit sub and drill collar design, and measurement, sensors, and control system are all components of the rig sub-system. Upgraded design for each system was taken in consideration and checked for economic and technical feasibility.

Drilling rig structure was redesigned with the addition of several new methods of interpreting drilling conditions via various sensors. From the previous year's design, there was found to be a flaw with the mechanical system that allowed the traveling block to move vertically. The traveling block did not move freely due to a linear guide bar that was bent and caused excessive friction that in turn affects weight on bit measurements. To mitigate the issue of friction build up due to issues in linear rail alignment a design that can both support and easily align linear rails has been selected. This year's rig structure will be a cantilever design which will be relatively easy to construct and more simplistic to align all the components. What makes this a cantilever is that the motor, water swivel, torque transducer and drill string will be suspended and held in place by only a single vertical structure that has horizontally protruding mounting plates. A cantilever is practical for applications that will not incur excessive bending moments, making it a suitable choice for this competitions purposes. Friction due to O-rings was also found to be a problem in the previous year's water swivel. In order to reduce the friction in the water swivel, the design has been modified to utilize shaft seals that allow the through shaft to spin freely with minimal friction. Having a water swivel that can rotate almost free of friction will allow the team to use a torque transducer to obtain dynamic torque readings.

Different drilling fluids have been studied for reducing friction while drilling and improve efficiency. PAC- based mud was found to be the optimum fluid for the operation needs. Pressure loss calculations were completed to provide information when setting up the circulation system to determine the optimum flow rate with sufficient hydraulic pressure and transport cutting ratio.

Theoretical analysis of vibrations has been made in order to optimize drilling process. Several challenges were faced during last year's competition. Due to misalignment of structure, drillstring mass imbalance and uneven height of PDC bit cutters, the drillstring experienced high vibrations resulting in failure at the brass tool joint of the drillpipe. It was hard to start the hole without minimizing walking and wobbling

tendency. Therefore, a guide shoe was used in order to guide the bit in the beginning of the drilling process. High friction increased bending, buckling and lateral vibrations tendency especially at higher rotational speeds. Different models were used to predict vibrations behavior of the drillstring and bottomhole assembly. Natural frequency at which the drillstring will resonate was determined using finite element method. Results obtained from theoretical and experimental analysis of vibrations will be used to upgrade the drilling control algorithm. Critical rotational speed will be avoided to reduce vibrations' amplitude. The rig structure will be constructed such that everything aligns as perfect as possible to reduce friction that can induce lateral vibrations.

Bit sub which also acts as a stabilizer has been designed in order to counter the deviation from the inclined rock planes. Welded blades, ball bearing and ball bearing cages are considered for the stabilizer design. A ball bearing cage will be slided on to the bit sub to reduce friction and allow free motion of the assembly. The allowed weight of bit sub is fixed at 20 pounds. Keeping the drillstring in tension avoids buckling tendency. A detachable weight can be screwed onto the bit sub to add weight on bit and create tension in drillpipe. A constriction has also been designed inside the bit sub to provide hydraulic force in case the weight has been unscrewed.

In terms of the automation of the design, some of the previous year's sensors were kept because of their excellent performance. However, the rest of the sensors were replaced with more efficient and appropriate sensors. Moreover, since this year's competition is more likely to have an inclined formation, more sensors were incorporated in the automation design. The reason behind that is to know the orientation of the bit in real time to maintain a vertical hole. The automation of the rig depends mainly on analog input and output, in order to simplify the system and decrease the number of components. One problem that was faced in last year's design was due to electric/magnetic interference that the equipment experienced, which made some sensors obsolete or inaccurate.

Controlling the linear motion of the actuator will be the same components as was used in the previous year's drilling rig. A torque transducer will be connected to the motor shaft and to the top shaft of the water swivel using couplings. Placing the torque transducer axially in line with the drill string will allow the team to obtain the most accurate measurements of torque. The real time measurements will then be fed into an updated version of the previous year's drilling algorithm to interpret the optimum weight on bit and rpm to be used. The algorithm optimize rpm while avoiding drillstring mechanical failures.

Weight on bit (WOB) is a crucial measurement that is required to properly regulate the pneumatic cylinder via measurements taken from the load cell and ran through the drilling algorithm. To control the WOB, the load cell is placed between the pneumatic piston knuckle and the traveling block. The previous

year's weight on bit measurements were also affected by the pneumatic cylinder chosen to actuate the traveling block. Weight on bit measurements were affected because the cylinder was too robust for the design and has O-rings that have a high friction coefficient. Therefore, this year, the team will be utilizing a much smaller pneumatic cylinder that has O-rings that are designed to have less friction allowing the piston to move more freely.

1. Drill Rig Traveling Assembly/Structural Design.

1.1 Previous Year's Design/Areas to Improve

The drill rig's structure and vertical traveling assembly was a key point of redesign for the 2015-2016 competition season. The reasoning behind this new initiative can be attributed to several mechanical issues with the previous year's design. In the previous design the bearings and linear guide rail of which the traveling block rode on were slightly out of alignment. This leads to an increase in friction as the traveling assembly traverses axially along the length of the derrick. The previous year's flaws was a result of last minute changes in design with limited time to make corrections. Through an examination of the previous year's rig, and discovery of a misalignment within the traveling assembly, an alternative plan was then initiated. In order to remedy this problem for the upcoming competition, a new design of the traveling block and rig structure was considered the best option.

1.2 Structural Design

It is integral to properly support and hold the linear motion system in alignment in order to achieve a reduction in friction, therefore providing a structure which can properly brace the linear motion system is necessary. Several designs were taken into account to be evaluated for ease of assembly and structural integrity. An A-Frame design was taken into consideration and evaluated upon cost and weight in comparison to other designs. In **Fig. 1** is the initial design that was primarily chosen due to its utilization of the same principles that were used in the previous year's design. However, the A-Frame was not chosen due to its complicated nature of construction in aligning the linear guide rails. In addition, the design of the A-Frame is heavier than the alternative design, weighing in at more than 300 pounds. The increased weight will cause rig to become too cumbersome for transport and operation.

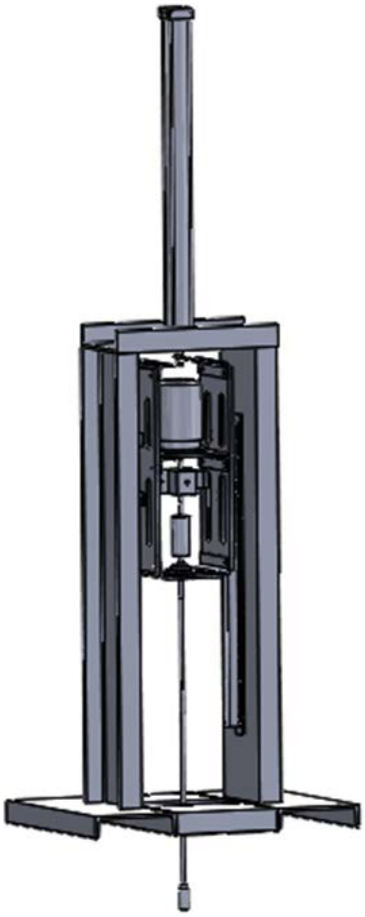

Fig. 1— A-Frame Design

Additionally proposed was a cantilever design in which the traveling block would cantilever out from a single vertical structural member. In **Fig. 2** is a caption of the chosen rig design for the 2015-2016 Drillbotics competition in its reclined position ready for transport. In this position the rig is under the 6 foot allowable limit and can fit through door ways to be showcased in a classroom setting. Casters on each leg allow the rig to have full mobility to be positioned wherever the operator feels it is convenient. As illustrated in Fig. 2, the rig will have all the electrical components compartmentalized within the electrical cabinet, and a water pump that will circulate fluid to the bit.

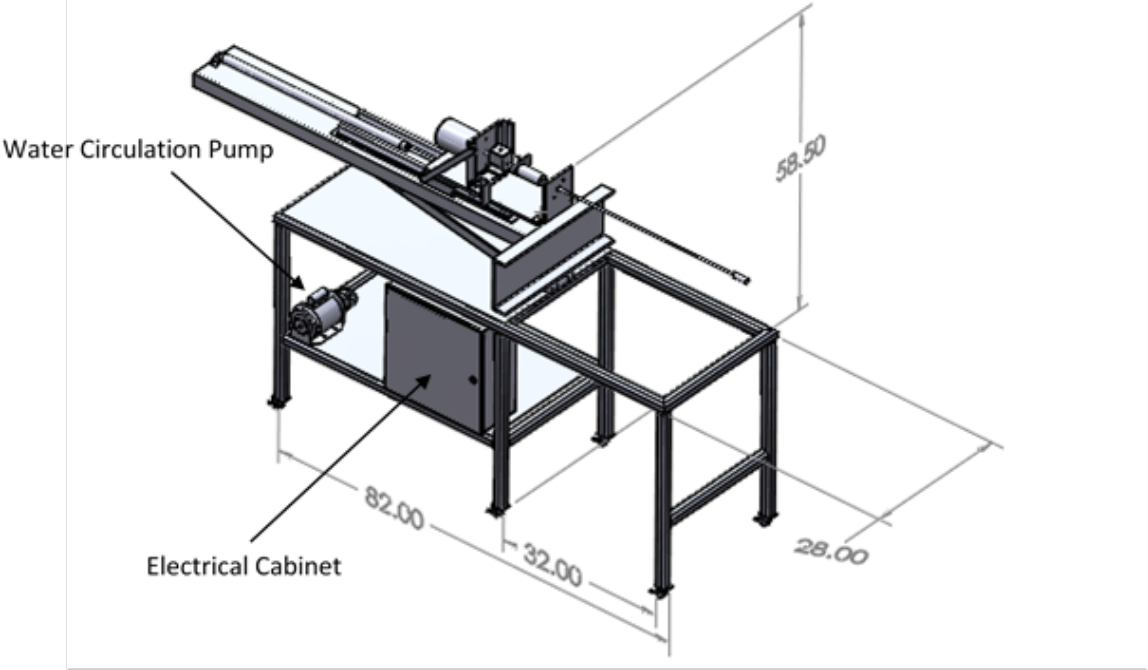

Fig. 2— Reclined Derrick Configuration (measurement units is inches)

In the upright position as seen in **Fig. 3** the rig is capable of being erected within a room that has 10 feet of clearance. This will further allow the rig to be used for educational purposes due to its mobility and low profile. The 32 inch gap between the legs under the drilling rig provides ample room for the 1 cubic foot drilling sample provided by DSATS.

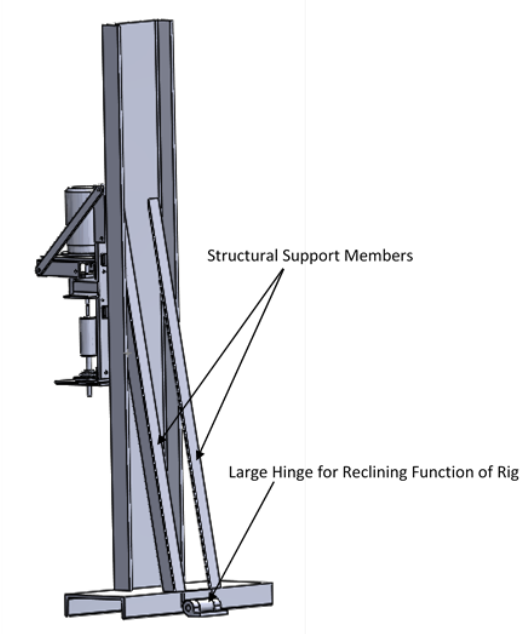

Fig. 3— Structural Supports for Cantilever Design

This design would require half the material as the A-Frame design and is much simpler to align the traveling assembly than using an A-Frame design. A cantilever can be unstable if not properly constructed using braces to minimize flex in the structure. The support structure will be supported with support members that will provide rigidity to the design. Due to the simplicity of design the cantilever approach has been selected as the final structural design (**Fig. 4**) for the 2015-2016 design competition.

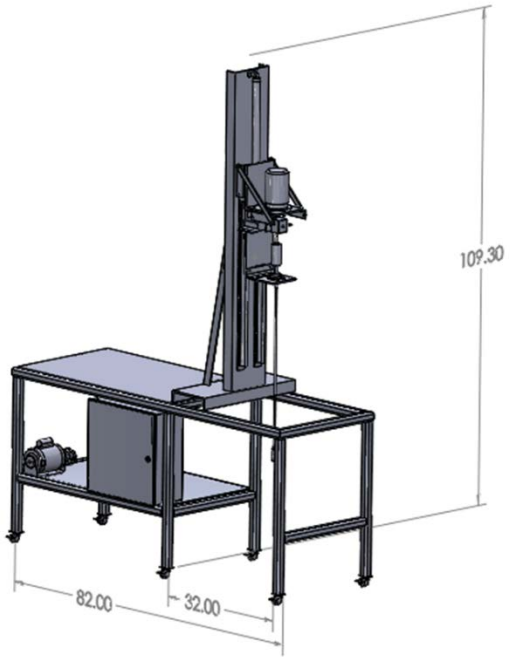

Fig. 4— Erected Derrick Configuration (measurements units is inches)

1.3 Traveling Block Assembly

The traveling block assembly will be much like the previous year's design where there is a traveling block attached to a pneumatic piston moving axially on the vertical support. Although as an alternative to mounting the cylinder directly above the traveling assembly it will be between the linear guide rails working in the same fashion as before but taking up less space vertically, minimizing the vertical height when erected. The Pillow blocks seen in **Fig. 5** will support the traveling block and allow the traveling block to move axially along the derrick. Using linear guide rails in conjunction with the pillow block bearings allow the traveling block to move axially with less friction than what was incurred in by the previous year's design. A round rail system was chosen because the tolerance allowed for miss alignment is greater than that of a square rail system. This allows the team a little room for error when constructing the rig.

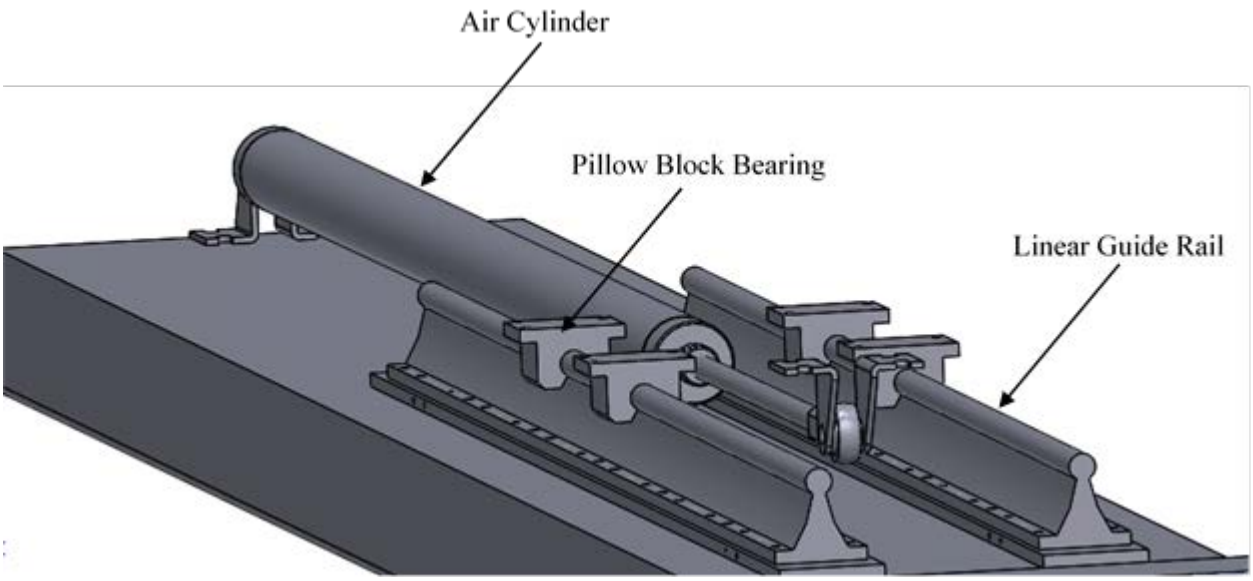

Fig. 5— Linear motion Equipment

The motor, water swivel, torque sensors and load cells will all be mounted to the traveling block that is attached to the pillow block bearings. A face mount motor was selected this year in order to easily centralize the motor and align the drive shaft with the thrust bearing that is concentric with the water swivels shaft. Placement of the torque transducer between the swivel and the drive shaft is due to the inability of the torque sensor to pass water through its shaft for circulation through the drill string. In order to get accurate readings from the torque transducer, the swivel was redesigned this year due to the friction in the seals not allowing the swivel shaft to rotate freely. For this year a swivel with shaft seals will be used to reduce friction and aid in allowing the torque transducer to pick up minute changes in torque while drilling. The traveling block will be machined out of 3/8 inch aluminum bar stock and will be used to mount the cantilevered instrumentation and drilling equipment. Secured to the derrick will be the linear guide rails that are aligned parallel to one another. Utilizing two guide rails mounted parallel to one another will provide the necessary support to prevent unwanted movement that is not axial to the derrick support structure.

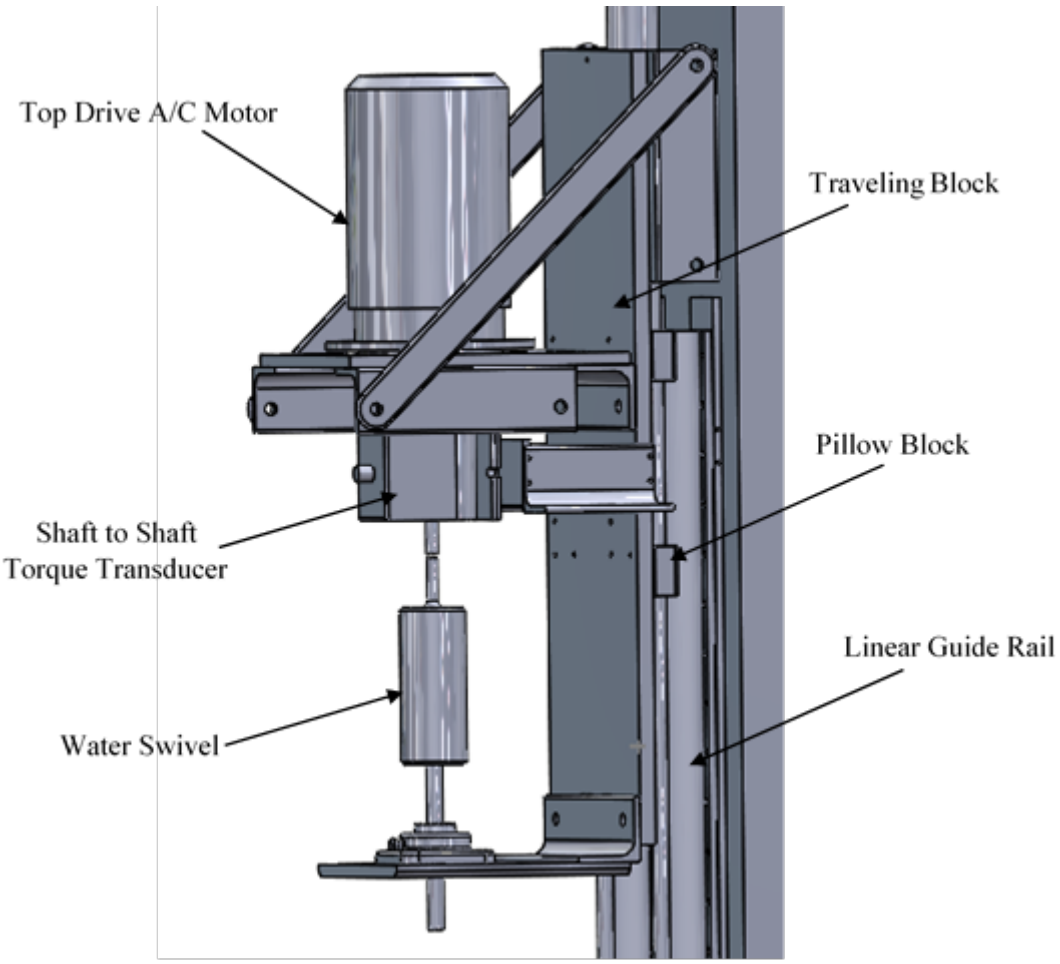

Fig. 6— Traveling Block Components and Assembly

1.4 Materials and Cost Analysis for Rig Construction

Materials taken into consideration for this year's rig construction include the use of either aluminum or steel for the structural members. The decision to choose one over the other is contingent upon the cost for both selections and the weight in comparison to one another. Thus a pricing and weight analysis was conducted to determine the benefits that could be gained using either steel or aluminum. A decision was made to use aluminum as the construction material because of the benefits in weight reduction. The cost of aluminum construction materials has a 16% increase in cost in comparison to steel, although the weight is reduced by 290% from 217 lbs. using steel to 75 lbs. using aluminum. This dramatic reduction in weight with little increase in price is the reason for why aluminum was selected as the design material. By reducing the weight, the rig becomes more mobile, simpler and safer to erect and recline the derrick.

Table 1— Cost and Weight Analysis for Steel and Aluminum Construction

Metal	Length Required	Purchased Length	Cost	Density	Structural Weight
	ft	ft	$	lb/ft	lb
2" x 2" x 1/4"Angle	12.6	20	49.2	3.19	40.2
10" x 2-1/2" x .24" C-Channel	8.1	10	168.3	15.3	123.9
8" x 3/8" Plate	3.4	6	247.86	10.2	34.7
2" x 1/4" Bar	8.7	12	45.84	1.7	14.8
1/4" x 1 -1/4" Bar	2.83	6	10.5	1.06	3.0
1/4" Brass Rod	2	2	5.36		
Total			$ 527.06		216.6
Plus 20% Contingency Cost Total			$ 632.47		

Aluminum Structure Cost and Weight Analysis					
Metal	Length Required	Purchased Length	Cost	Density	Structural Weight
	ft	ft	$	lb/ft	lb
2" x 2" x 1/4"Angle	12.6	25	99.75	1.11	14.0
10" x 2-1/2" x .24" C-Channel	8.1	12	356.4	5.28	42.8
8" x 3/8" Plate	3.4	6	129.6	3.52	12.0
2" x 1/4" Bar	8.7	12	26.04	0.57	5.0
1/4" x 1 -1/4" Bar	2.83	6	8.8	0.36	1.0
1/4" Brass Rod	2	2	5.36		
Total			$ 620.59		74.7
Plus 20% Contingency Cost Total			$ 744.71		

Utilizing aluminum for the construction phase will also make machining and fabrication easier due to the qualities inherent to aluminum and its easy machinability. The cost for linear and rotating equipment has been outlined in **Table 2** with 20% contingency costs included.

Table 2— Cost Analysis of Linear Motion and Rotating Equipment

Linear Motion and Rotating Equipment			
Description	cost ea. $	quantity	cost, $
1/2" x 48" Linear Rail W/mounting Plate	231.2	2	462.4
1/2" Linear Pillow Block	121	4	484
1-1/4" X 36" Air Cylinder	140	1	140
7/16" Tie Rod Ball Joint End	5.8	1	5.8
1- 1/4" Pivot Bracket	8	1	8
Leeson 1/4hp 50Hz 3 Phase C-Face motor	245	1	245
Total			$1,345.20
Total Cost plus 20% Contingency			$1,614.24

2. Circulation system

The primary objectives of the circulation system involve cooling, lubricating the drilling bit, and cutting transport from the wellbore. There are several factors that are taken into account when selecting the most ideal circulation system, with the most prominent factors being cost and performance. The main types of drilling fluid used are the freshwater, water-based mud, oil-based mud and foam. The circulating fluid that will be used in this system is PAC based drilling fluid instead of tap water, because the coefficient of friction (COF) of PAC based mud is 0.40, which is less than the COF of water that is 0.70. It is essential to reduce the frictional force between the drill string and the wellbore, which can increase or sustain the desired ROP with increase in the hydraulic pressure. It is vital to note that the structure of the rig will include the installation of a pump. The mode of operation for a pump is relatively simple; the process involves the flow of PAC drilling fluid via from the tank through PVC pipe, hose and the swivel and down the drill pipe and up the annulus. Also, there will be flow nipple at the top of the concrete block surrounding the drill pipe, so the PAC fluid and cuttings flow to sieve and back into the tank. The PVC pipe will go up to the derrick top and then hose will be connected to the swivel in a loop pattern that is suitable for the movement of swivel along with the traveling block. The fluid will be recirculated back to the sieve and then to the collector tank. After, the drilling process the PAC based fluid will be recycled.

It is also vital to consider pressure loss calculations when setting up the circulation system. These pressure losses are seen in the drill pipe, annulus, bit nozzles as well as minor components such as pipes and fittings. In order to determine the flow rate that will provide sufficient cutting transport ratio and hydraulic pressure which is based on the pressure rating of the pump (300psi), calculations were done at different flow rates and different wall thickness of the pipe.

2.1 Pressure loss calculations

Pressure drop across the system was calculated using PAC based drilling fluid to estimate the flowrate and pressure rating needed for the pump for circulation system. The PAC based fluid is a power-law fluid. This fluid possess the behavior of non-Newtonian fluid.

Based on the guidelines, Round Aluminum tube will serve as the drill pipe and this tube have different wall thickness (different inside diameter). Based on the calculation, we decided to go for 0.277 inches for the inside diameter, which can deliver high hydraulic pressure compare to other two inside diameter in the guidelines and circulate the cuttings at the flowrate of 7 gallon per minutes. **Table 3** has the specifications and parameters used for the pressure loss calculations.

Table 3— Parameters for pressure loss calculations

Q, gpm	7	K(lbf.s^n/ft^2)	62.3	ρ_{Pac}, ppg	8.32	L_{bit}, in	4.758
OD_{pipe}, in	3/8	N	0.6120	OD_{bit}, in	1.125	L_{hose}, ft	18
ID_{pipe}, in	0.277	D_{nozzle}, mm	2.35	ID_{bit}, in	57/128	OD_{hose}, in	0.5
C_d	0.95	Nozzles	2	L_{pipe}, in	36		

2.1.1 Pressure drop in the pipe

The average velocity of the fluid was calculated using **Eq. 1** and found to be equal to 37.267 ft/s or 11.359 m/s.

$$V = \frac{q}{2.448\left(ID_{pipe}^2\right)} \quad \text{..... (1)}$$

Reynolds number was calculated based on SI unit of each dependent parameters. Then, the shear stress at laminar flow of the pipe wall is calculated using **Eq.2** and substituting zero 0.612, and 0.478 for power law fluid yield stress (T_y), power index (n), and consistency index (k) respectively. The shear stress at laminar flow (T_{wlam}) was found to be 171.607 Pa.

$$T_{wlam} = T_y + K\left(\left(\frac{3n+1}{4n}\right)\left(\frac{8v}{D}\right)\right)^n \quad \text{..... (2)}$$

Reynold's number was calculated using **Eq.3** by substituting results from Eq.1, Eq. 2, and a density of 997.95 kg/m^3. The calculated Reynold's number was 6002.7. Since Reynold's number is larger than 4000, the flow is turbulent. The friction factor is calculated using **Eq.4** (Dodge 1959). Substituting 0.623 for N, the friction factor was found to be 0.00655. Excel's goal seeker was used to solve Eq.4 since it is an implicit equation.

$$Re = \frac{8\rho U^2}{T_{wlam}} \quad \text{..... (3)}$$

$$\frac{1}{f^{0.5}} = \frac{4}{N^{0.75}}\log\left[Ref^{\left(1-\frac{N}{2}\right)}\right] - \frac{0.4}{N^{1.2}} \quad \text{..... (4)}$$

Shear stress (T_w) that accounts for the friction factor was calculated using **Eq.5**. Using SI units, Eq.5 results in T_w equal to 421.53 Pa.

$T_w = 0.5(f)(\rho)(U^2)$ ……..……..…. (5)

The pressure loss of the pipe was calculated using **Eq.6**. Setting l equal to 3 ft, pipe pressure loss is equal to 31.783 psi.

2.1.2 Pressure loss in bit

The pressure loss in the bit was calculated using Eq. 6 in similar fashion as pipe pressure loss. Assuming mud weight (MW) of 8.32 ppg, the pressure loss in the bit is equal to 0.4448 psi.

$dP_{pipe} = \frac{4T_w l}{D}$ ……..…….…..…. (6)

2.1.3 Pressure drop in annulus

The annular velocity was calculated using Eq.1 and subtracting $(OD_{bit})^2$ from $(OD_{pipe})^2$ in the denominator. The annular velocity is equal to 2.542 ft/s or 0.775 m/s. Assuming T_y is equal to zero, annular T_w can be calculated using **Eq. 7** and is equal to 23.752 Pa. Reynold's number in the annulus was calculated to be 201.739 using Eq. 3. The flow is laminar since Re is less than 2300. Than annular pressure drop was found to be 0.6614 psi using Eq. 6. It should be noted that the pressure loss in the annulus calculations were based on the assumption that the drill pipe will form concentric annulus. The diameter of drilled hole is assumed to be the same as the diameter of the external diameter of the bit. The annulus length is taken as 36 inches.

$$T_w = \left(\left(\frac{12v}{OD_{bit} - OD_{pipe}} \right) \left(\frac{K^{\frac{1}{n}}(1+2n)}{3n} \right) \right)^n \quad \text{..... (7)}$$

2.1.4 Pressure loss in the nozzles and hose

The bit have two nozzles each with diameter of 2.35mm (0.0925 in). The area of the nozzle was calculated using **Eq. 8** and found to be equal to 0.031446 in^2. Assuming a discharge coefficient (C_d) of 0.95, pressure loss across the nozzle was calculated using **Eq. 9** and was equal to 207.66 psi.

Area of nozzle$= \frac{\pi}{4} \times 2 \times (OD^4)$ ……..…..…. (8)

$dP_{nozzle} = \frac{(MW)(Q^2)}{12032(C_d^2)(A^2)}$ ……..…….. (9)

The pressure loss in the hose was calculated using Eq. 6 in similar pattern as pipe pressure drop calculations and it is equal to 14.54 psi. Therefore, the total downhole head loss is 255.1 psi.

2.2 Summary

A circulation system is included in the design of an automated drilling machine in order to transport cuttings to the surface, lubricate and cool the bit as well as reduce the friction between the drill string and wellbore. PAC based drilling fluid will be used as the circulating fluid, which is easily accessible and can be prepared in the drilling laboratory. Also, it is capable of exerting sufficient hydrostatic pressure on the formation and deliver the desired flowrate.

3. Vibration Analysis and Control

Vibrations critically affect rate of penetration, the life of the drillstring, and bottomhole assembly. Therefore, effort to mitigate or prevent vibration is vital to optimize the drilling conditions. It is also possible to drill at higher RPM if vibrations are reduced. A better understanding of vibrations is significant to achieve the team's goal to mitigate vibration tendency. Research for a simple analytical model to analyze vibration was done throughout the semester. The focus of the research was on vibration types that were most likely to occur. Last years' experience was taken into consideration while choosing the most concerning vibration types. It was decided to focus on whirl and bending since they are expected to cause the most damaging vibrations.

3.1 Modal Analysis of Drillstring

A modal analysis determines the vibration characteristics (natural frequencies and corresponding mode shapes) of a structure using Finite Element Analysis (FEA). FEA divides a system or structure into smaller elements of a mesh with nodes to mathematically model and numerically solve complex structural and fluid problems. The natural frequencies and mode shapes are important parameters in the design of a structure for dynamic loading conditions. Natural frequency is the frequency at which the system vibrates in its ideal state. When a force is applied, the frequency of vibration is equal to the frequency of the applied force. Mode shapes describe the configurations into which a system or structure will naturally displace itself. The number of natural frequencies and mode shapes depends upon the number of frequencies and the unconstrained mesh points in a Finite Element model. Finite Element models have a large number of natural frequencies and mode shapes but only the smaller frequencies will be accurate and useful for any practical applications.

If the frequency of the applied force is equal to the natural frequency of the system then the amplitude of vibration increases substantially and the phenomenon of resonance occurs. Larger amplitude of vibration creates larger deformation of system. Thus, whenever a system is designed, the frequency of the applied force is always kept less than that of the natural frequency. Ansys Workbench 16.1 software was used for

modal analysis of the drillstring. A structural model of the drillpipe was created in the Mechanical application and Modal section was run for the model (**Fig. 7**). The results are shown in **Table 4**.

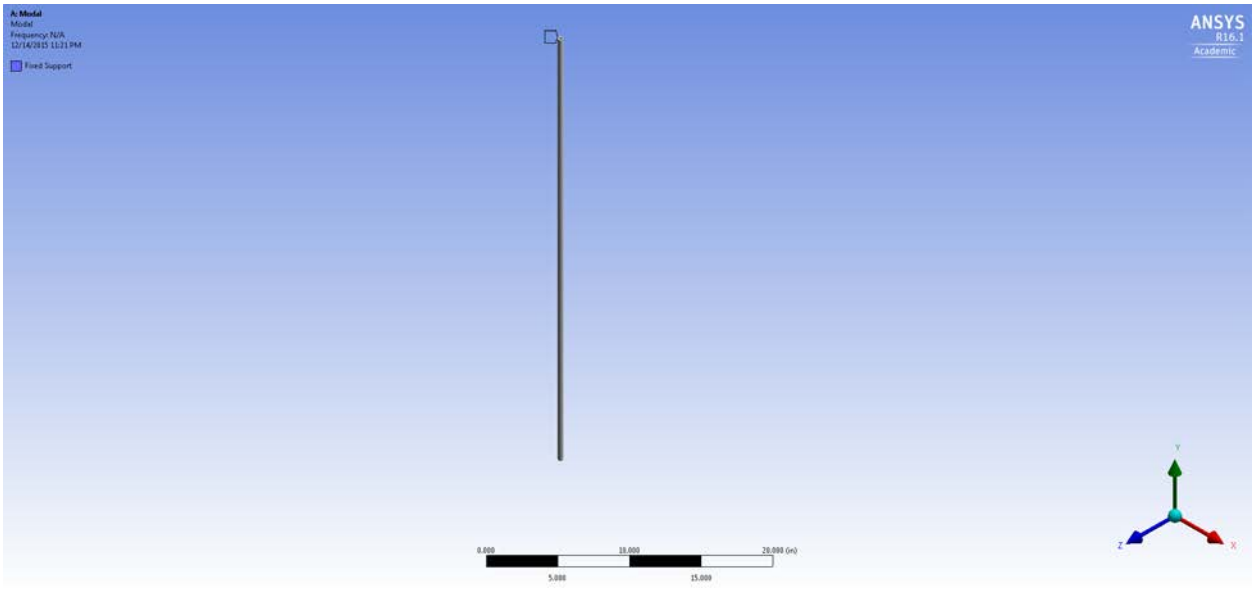

Fig. 7— Drillstring Modelling in Ansys Workbench

Table 4— Result from Modal Analysis of Drill Pipe

Mode	Frequency [Hz]	RPM	Mode	Frequency [Hz]	RPM
1	10.904	654.24	6	190.88	11452.8
2	10.907	654.42	7	373.09	22385.4
3	68.265	4095.9	8	373.18	22390.8
4	68.281	4096.86	9	614.91	36894.6
5	190.84	11450.4	10	615.05	36903

The natural frequency of the drillpipe given in the guidelines which has 3/8” outer diameter with 0.016” thickness and made of aluminum alloy 6061 is 10.904 Hz. If the frequency of the applied force is equal to 10.904 Hz then resonance will take place increasing the amplitude of vibrations leading to a failure of the drill pipe. It implies that if the drill pipe is forced to rotate at a frequency of 10.904 Hz or 654 rotations per minute then the pipe may fail due to excessive vibrations. The first and second modes are almost equal. Using the above results we will not rotate our drillpipe at 654 RPM to avoid excessive vibrations.

Similar modal analysis was carried out for the bit sub described in **Fig. 17** and the results are shown in **Table 5**. As the natural frequency is very high, there is no need for any caution to operational parameters.

Table 5— Result from Modal Analysis of Bit Sub

Mode	Frequency [Hz]	RPM
1	2808.6	168516
2	2808.6	168516
3	10270	616200
4	11600	69600
5	11646	69870
6	12722	76322

3.2 Whirl

Lateral displacement is negligible when the center of drill string rotation coincides with the center of the hole. However, when center of rotation is offset from the center of the hole, the drill string walks around the hole as it is rotating around itself. Whirling can be a result of bit vibration and misalignment of the drillstring and bottomhole assembly. Whirl is destructive to the drillstring and bottomhole assembly and causes rapid fatigue to connections (Dykastra et al. 1996).

Four types of whirl exist: forward synchronous, forward with slip, backward with slip and backward without slip. Forward whirl happens when the drillstring walks in the same direction as the rotation while backward whirl occurs as the drillstring walks against the direction of rotation due to increase in friction (Vandiver et al. 1990). Drillstring is assumed to be rotating in clockwise direction (negative direction). Therefore, forward whirl rate has a negative sign while backward whirl rate is positive. The maximum forward whirl rate occurs when the rate is equal to drillstring rotation. Meaning that the maximum whirl rate will be when there is a forward synchronous whirl. The drillstring will be in continuous contact with borehole wall and hence surface of drillstring can be eroded. However, bending stress rate on the drillstring will be equal to zero for forward synchronous whirl (Vandiver et al. 1990). Backward without slip whirl rate can be calculated using **Eq.10**. Bending stress rate on the drillstring will be highest for backward non-slip.

$$\Omega_b = -\frac{r_{ds}}{r_b - r_{ds}} RPM \quad \text{..... (10)}$$

Whirl range can be plotted against slip velocity at a constant RPM. Slip velocity is calculated using **Eq.11** and **Eq.12** and it is highest for forward synchronous whirl ($v=r_b*\Omega_b$) and lowest for backward non-slip whirl (v=0). **Fig. 8** and **Fig.9** show the theoretical whirl range at critical RPM of 650 for the drillstring

and the stabilizer respectively. Due to much smaller stabilizer clearance, backward non-slip whirl is significantly higher than drillstring backward non-slip whirl.

Since only 12 in will be drilled the day of the competition, stabilizer whirl range will only be taken into account as the stabilizer will dominate vibration behavior. Backward whirl is expected due to high friction; however, expected whirl range will be further analyzed during the testing phase.

$$F_s = \frac{\Omega}{\Omega_b} . \quad (11)$$

$$v = (r_b - r_{ds})\, F_s\, \Omega_b + r_{ds}\, RPM \quad (12)$$

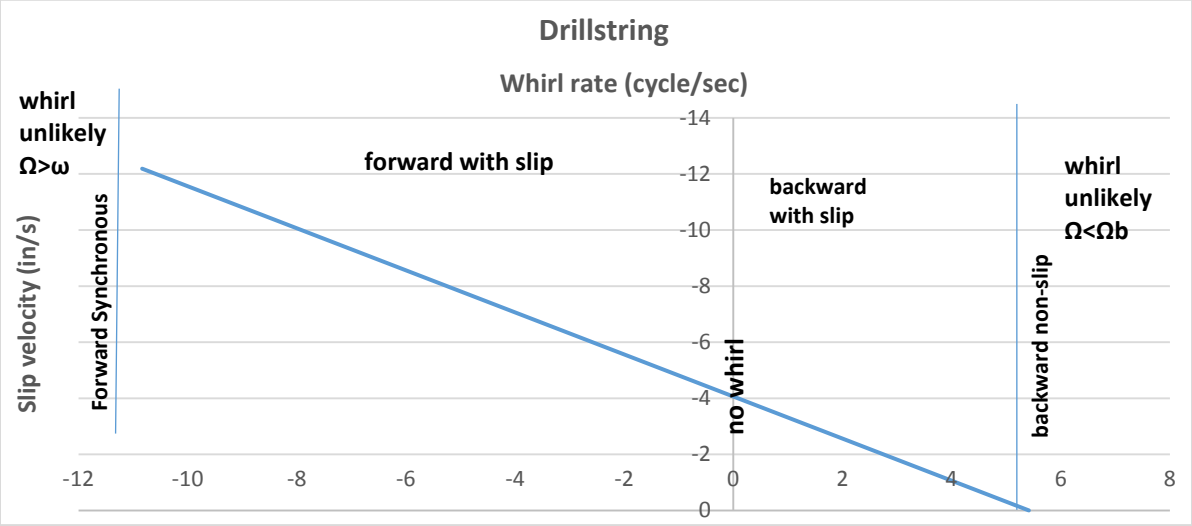

Fig. 8— Slip Velocity versus Whirl Range at 650 RPM for the Drillstring Alone

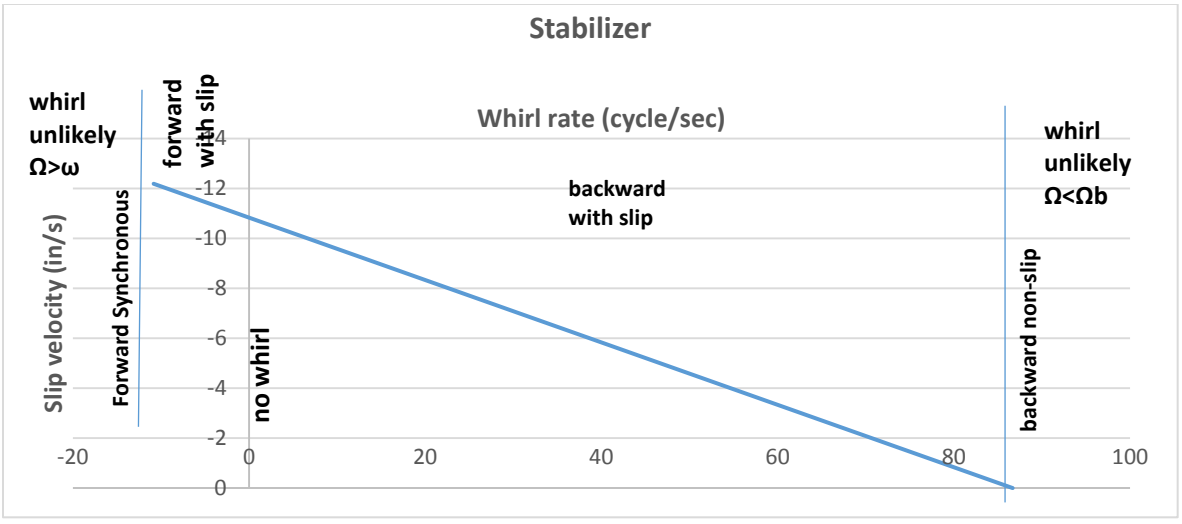

Fig. 9— Slip Velocity versus Whirl Range at 650 RPM for the Stabilizer

Bending stress and bending moment are expected to increase due to deflection caused by whirl. While drilling, bending stress can be measured from load cells. Bending stress can be calculated using **Eq. 13**. Phase angle is the arctangent of B_y/B_x and is related to whirl rate. Whirl rate can be determined from knowing the slope of phase angle versus time plot during transient time (**Eq. 14**). The slope will be zero in case of forward synchronous whirl.

$$\vec{B} = B_x\ \vec{i} + B_y\ \vec{j} = |\vec{B}|\{\cos(\alpha(t))\,\vec{i} + \sin(\alpha(t))\,\vec{j}\} \quad (13)$$

$$\alpha(t) = arctan\left[\frac{B_y(t)}{B_x(t)}\right] + \alpha_0 = (\Omega - \omega) + \alpha_0 \quad (14)$$

During testing phase, the team will be able to get more information about the expected bending stress and phase angle. Whirl range can be calculated from knowing the values of bending stress and phase angle.

For the theoretical analysis, bending stress can be calculated assuming a constant WOB of 20 lb. Bending stress can be calculated using **Eq.15**. The free body diagram is shown in **Fig.10**. The values and location of maximum shear force and bending moment can be determined using Shear and bending moment diagrams. In order to plot shear and bending moment diagrams, all variables (fx_1, fx_2, fx_3 and M) should be determined by solving a system of equations. Phase angle (**Eq.14**), radius of curvature (**Eq.16**), and deflection (**Eq.17**) will be determined once bending moment components (B_x, B_y) are calculated. The analysis will be completed during the second phase of the competition. The system of equations to be solved is shown in **Eq.18a**, **Eq.18b, Eq.18c** and **Eq.18d.**

$$\sigma = \frac{F}{A} + \frac{M\,C}{I} \quad (15)$$

$$\frac{1}{\rho} = \frac{M}{E\,I} \quad (16)$$

$$\theta = \frac{L}{\rho} = \frac{L+\Delta L}{\rho+c} \quad (17)$$

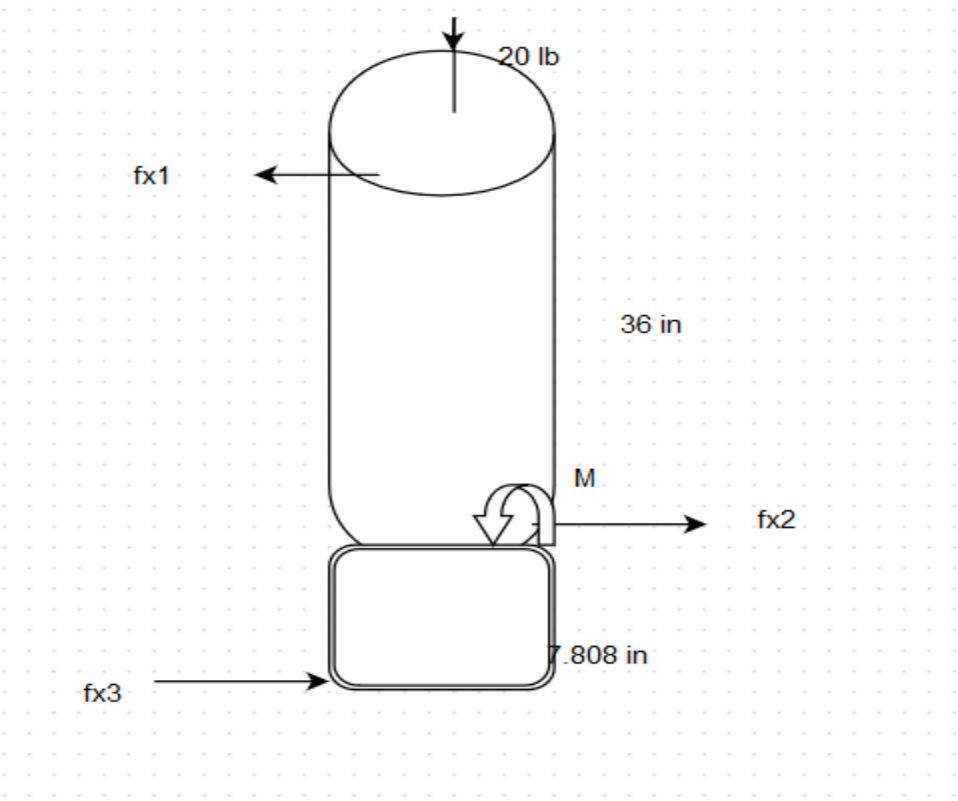

Fig. 10— Free Body Diagram of the System. Applied WOB=20 lb. Fx1: Swivel Side Force. Fx2: Stabilizer Side Force. Fx3: Bit Side Force. M: Bending Moment

$M + 43.808\, f_{x1} - 7.808\, f_{x2} = 0$ ..... (18a)

$M + 36\, f_{x2} + 43.808\, f_{x3} = 0$ ..... (18b)

$M + 36\, f_{x1} + 7.808\, f_{x3} = 0$ ..... (18c)

$f_{x1} = f_{x2} + f_{x3}$ ..... (18d)

3.3 Forced Frequency Response:

Vibrations can be analyzed using forced frequency response function. Harmonic excitation for undamped mass-spring system was used to predict vibration behavior at a critical RPM of 650. Equation of motion is shown in **Eq.19**. Solving the differential equation in Eq.19 and substituting natural frequency (**Eq.20**) results in **Eq.21** (Apostal 1990). When damping viscous fluid is introduced to the system, damped mass-spring system will be used in forced frequency response analysis. The reason undamped system was used to predict vibration is that the team hasn't finalized the hydraulics yet. However, a damped system will be taken in to consideration during the construction phase once hydraulics has been finalized. Equation of motion will be adjusted for a damped system (**Eq.22)**.

$F_0 \cos(\omega t) = k\, x + m\ddot{x}$ ..... (19)

$$\omega_n = \sqrt{\frac{k}{m}} \quad \text{..... (20)}$$

$$\frac{F_0}{m}\cos(\omega t) = \omega_n\, x_0 \cos(\omega t) - \omega^2\, x_0 \cos(\omega t) \quad \text{..... (21)}$$

$$F_0 \cos(\omega t) = k\, x + b\dot{x} + m\ddot{x} \quad \text{..... (22)}$$

The excitation factor in this model is assumed to be a function of bit type. Frequency of the vibration which indicates whirl rate is dependent on the excitation factor and rotary speed (**Eq.23**). Excitation frequency for a tri-cone bit is equal to 3*RPM. Equivalent blade affects excitation factor in PDC bit. Since the team will be using a PDC bit, equivalent blade was calculated using **Eq. 24** and **Eq.25** (Peterson 1976). Total diamond penetration, P, was assumed to be one sixth of diameter of diamond, d_d (Peterson 1976). Equivalent blade for the bit that will be used in the competition was calculated to be 0.855. Therefore, excitation factor and frequency at 650 rpm are 0.855 and 9.26 cycle/s, respectively.

$$\omega = EF * \frac{RPM}{60} \quad \text{..... (23)}$$

$$b = 2 * \sqrt{d_d P - P^2} \quad \text{..... (24)}$$

$$n_{eb} = 0.61 * 2 * b * \frac{n_{bs}}{d_b} \quad \text{..... (25)}$$

Assuming a constant WOB of 20 lb, predicted displacement, velocity and acceleration range was calculated by forced frequency response method using **Eq.26**, **Eq.27** and **Eq.28** respectively. Plots of displacement, velocity and acceleration versus rotational speed are shown in **Fig.11**, **12** and **13** respectively. The maximum value in each plot occurs at the critical rotational speed of 650 rpm (Irvine 1999).

$$\left|\frac{x(\omega)}{F(\omega)}\right| = \frac{1}{k}\left[\frac{\omega_n^2}{\sqrt{(\omega_n^2-\omega^2)^2+(2\xi\omega_n\omega)^2}}\right] \quad \text{..... (26)}$$

$$\left|\frac{v(\omega)}{F(\omega)}\right| = \frac{1}{k}\left[\frac{\omega\omega_n^2}{\sqrt{(\omega_n^2-\omega^2)^2+(2\xi\omega_n\omega)^2}}\right] \quad \text{..... (27)}$$

$$\left|\frac{a(\omega)}{F(\omega)}\right| = \frac{1}{k}\left[\frac{-\omega^2}{\sqrt{(\omega_n^2-\omega^2)^2+(2\xi\omega_n\omega)^2}}\right] \quad \text{..... (28)}$$

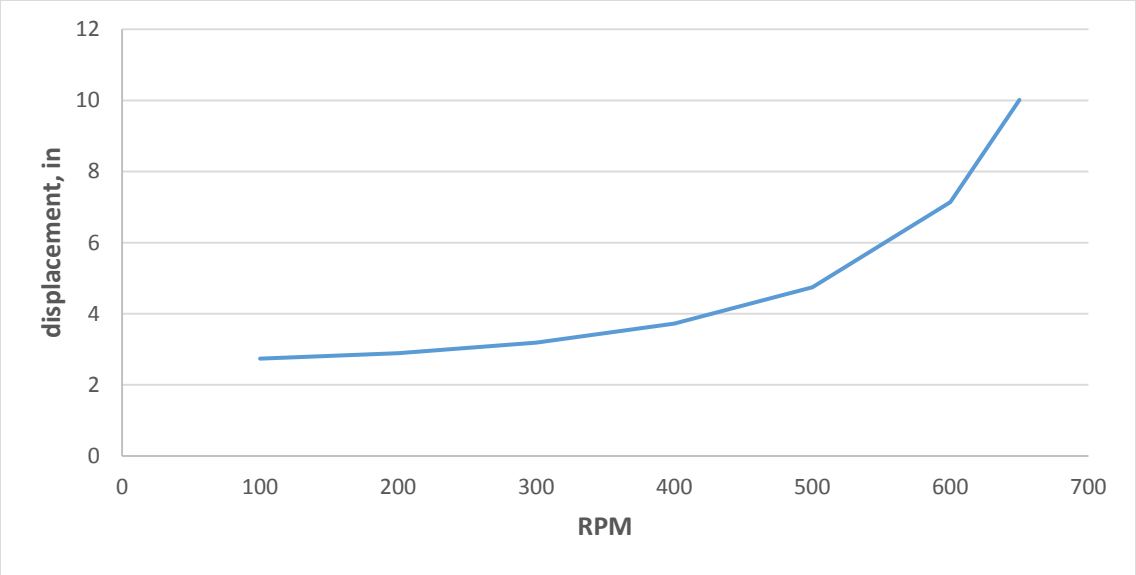

Fig. 11— Displacement versus RPM

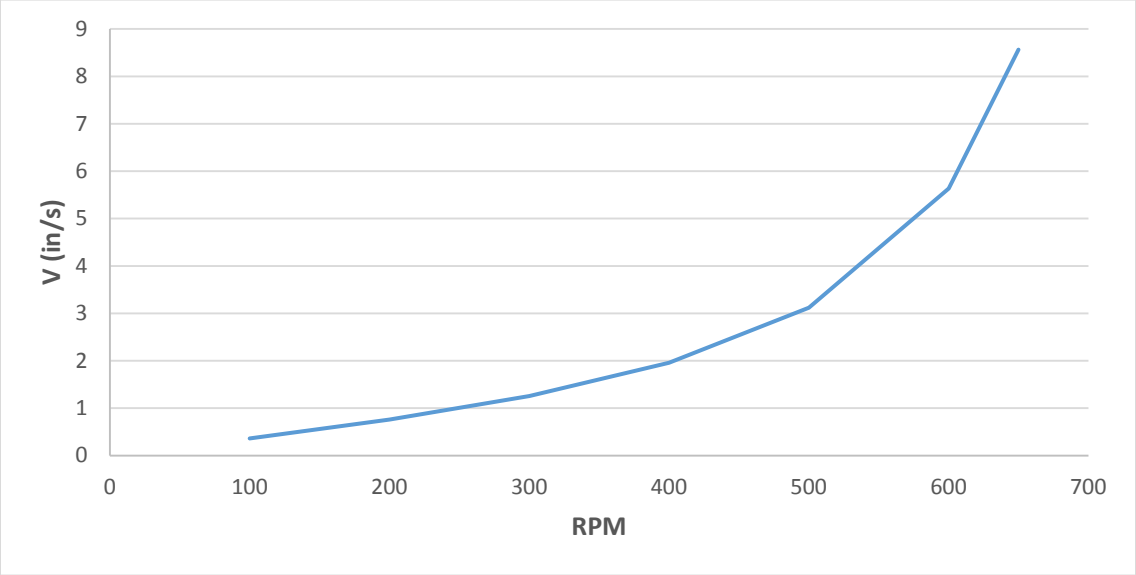

Fig. 12— Velocity versus RPM

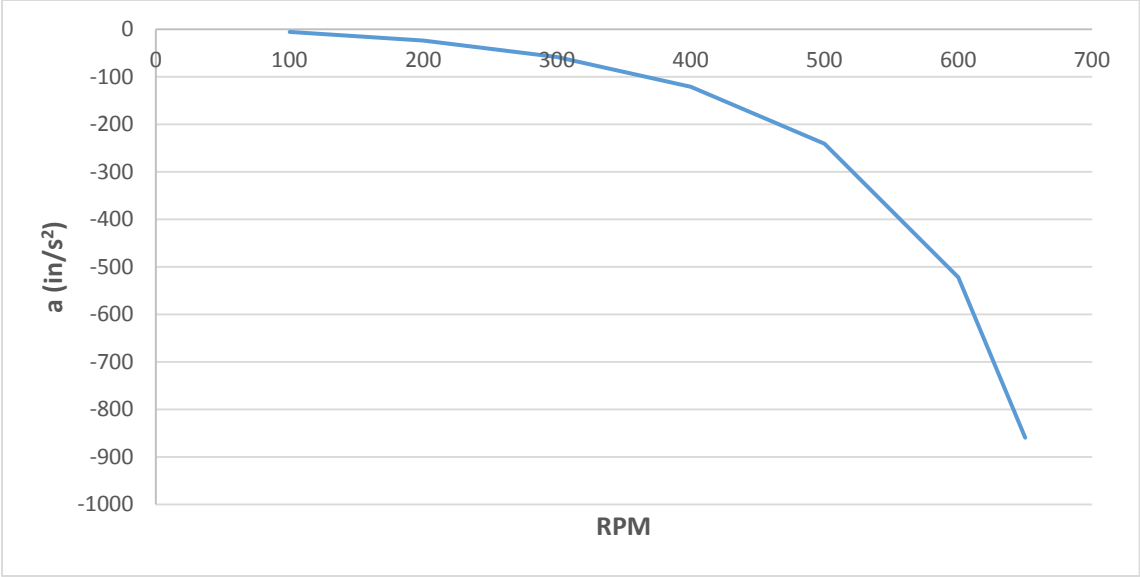

Fig. 13— Acceleration versus RPM

Assuming a total drilling time equal to one hour, displacement was plotted versus time at critical rotational speed of 650 rpm as shown in **Fig. 14**.

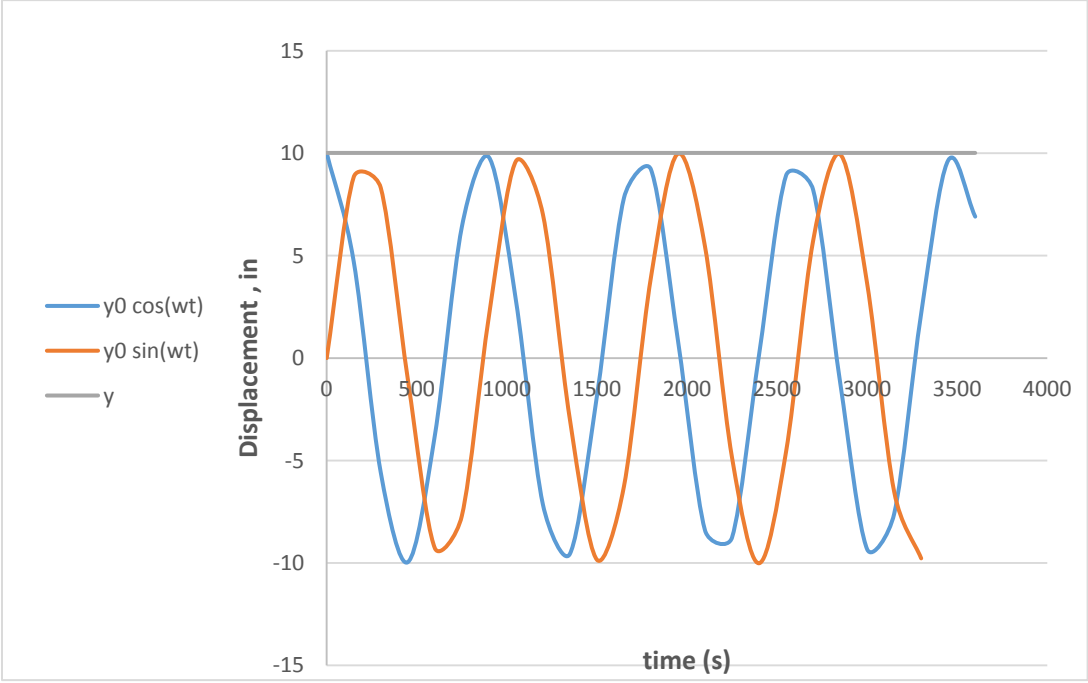

Fig. 14— Displacement versus Time at 650 RPM

3.4 Jansen model:

Whirl prediction was determined in Jansen model using forced frequency response and other complicated equations. Due to difficulties in solving such complicated equations and the lack of all variables needed, Jansen model will not be considered in predicting vibration (Jansen 1992).

3.5 Dykstra Model:

Drillstring imbalance can be inferred from **Eq.29** that gives the dimensionless whirl amplitude which represents the ratio of the shaft's radial deflection to its eccentricity. Whirl amplitude will increase until it reaches a maximum when rotary speed equals natural frequency (Ω_D =1). Whirl amplitude decreases when rotary speed exceeds natural frequency (Dykstra et al. 1996). The main limitation of this model is the inability to predict the actual drilling vibration behavior. However, this equation is useful to predict drillstring imbalance.

$$A_D = \frac{\Omega_D}{[(1-\Omega_D{}^2)^2+(2\,\xi\,\Omega_D{}^2)^2]^{0.5}} \quad \text{..... (29)}$$

3.6 Conclusion:

Theoretical and experimental analysis on vibration will benefit the team to optimize drilling parameters. Critical rotational speeds will be avoided during drilling. Also, an upgraded version of drilling control algorithm will be used to optimize rotational speed while avoiding drillstring failure. The algorithm controls WOB such that the RPM is maximized to enhance rate of penetration. The program will use inputs from sensors and will adjust speed and WOB as needed. Moreover, MSE will be considered during the testing phase and time of competition.

4. Bit Sub/ Drill Collar Design

Bit Sub is a piece of tubular with 2 box ends to connect the bit to the drill string. While a Drill Collar is thick walled to provide WOB and keep the drill string in tension. The length of the drill collars is designed such that the neutral point where all axial forces on the string are zero, is in the drill collars. For Drillbotics competition, a 3" long 3/8" NPT box down by 1/4" NPT box up will be provided as bit sub/drill collar. Throughout the report, "bit sub" includes drill collars unless otherwise specified. As per the guidelines, it is encouraged for the team to design and build their own bit sub. There are two limitations on the bit sub design. First, the maximum weight which can be attached is 20 lbs. Second, stabilizer should not stiffen the drillstring. Based on the guidelines following design of the bit sub have been proposed.

4.1 Stabilizer

Conventionally a stabilizer is used to keep the drill collars centralized to avoid unintentional sidetracking, vibrations, and quality of borehole. Different types of stabilizers are available in the market and the placement of stabilizers is dependent on the hole section being drilled. Building assemblies apply the fulcrum principle by placing a near bit stabilizer to force the bit on the high side of the borehole. Dropping assemblies apply the pendulum principle by placing a stabilizer far away from the bit causing gravity to pull the bit on the low side of the bore hole. For holding assemblies a packed hole assembly is used in which three to five stabilizers are properly placed to maintain the angle.

As per the guidelines, the simulated formations in the rock samples may not be parallel to each other. According to the theory, a packed hole assembly needs to be designed for maintaining a straight borehole. A stabilizer will be placed on the bit sub to create a packed hole assembly to prevent the bit from drilling in the direction of the dip. Following are the few designs proposed.

4.1.1 Welded Blades

The guidelines caution us that the stabilizer should not stiffen the drillstring, so we decided to design the bit sub of the same length as given by DSATS. A 3 inch long steel pipe with outer diameter of 0.75 inch and inner diameter of 0.64 inch will be machined out of a 0.75 inch thick steel bar. A 0.125 inch wide and 0.125 inch thick steel ring with rounded outer edges would be welded at the center of the bit sub to act as a stabilizer. This design will create more friction while rotation. Also continuous rotation at the same place may create a groove in the rock giving us misleading MSE numbers and will hinder further downhole motion. Hence this option is not selected.

4.1.2 Magnetic Casing

A magnetic casing was considered to stabilize the drillstring and minimize undesired deviation. The magnetic casing was planned to be placed around the drillstring without touching it as illustrated in **Fig. 15**. The reason behind that was to constrain the drillstring's trajectory and gain control over it. However, the main concern was the nonconductive aluminum drillstring. It was feared that aluminum will not be affected with magnetic field. However, it was still considered and researched in case the drillstring used became a steel drillstring. After researching the issue, it was found that the moving drillstring inside a magnet will induce a current in the drillstring. As a result the drillstring will acquire its own magnetic field, which will interfere with the magnets. The phenomenon is known as Eddy current which will create a braking effect on the drillstring no matter if it was made of aluminum or steel (Zhou et al. 2012). As a result, this option was eliminated.

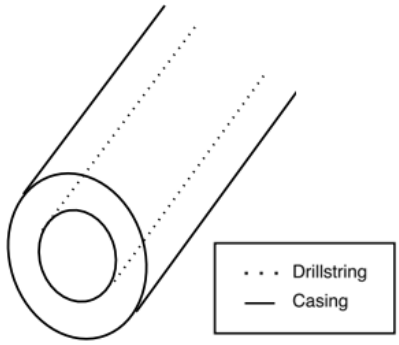

Fig. 15— Illustration of the Magnetic Casing Design

4.1.3 Ball Bearing

A 3 inch long bit sub with outer diameter of 0.375 inch and inner diameter of 0.275 inch is to be machined. A ball bearing of outer diameter 1 inch and shaft diameter of 0.37 inch with 0.3125 inch thickness is to be welded at the center of the bit sub acting as a rotating stabilizer. This should reduce the friction while drilling but will still hamper the axial motion of the drill string.

4.1.4 Ball Bearing Cage

The following design is inspired form the ball point pen design. The small ball bearing in the ball point pen rotates with minimum friction in any direction with minimum contact with the surface. On similar thought a ball bearing cage of length 3 inches will be attached on the outside of a bit sub with outer diameter of 0.75 inches and inner diameter of 0.64 inches. The ball bearings in the cage will allow free rotation of the bit sub with minimum wall contact and also allow smooth axial motion. Hence this design is selected for the stabilizer on the bit sub. The cage is around 2 inch long and 1 inch wide. The cost of the cage is 3 dollars.

Fig. 16— Ball Bearing Cage (Alibaba.com)

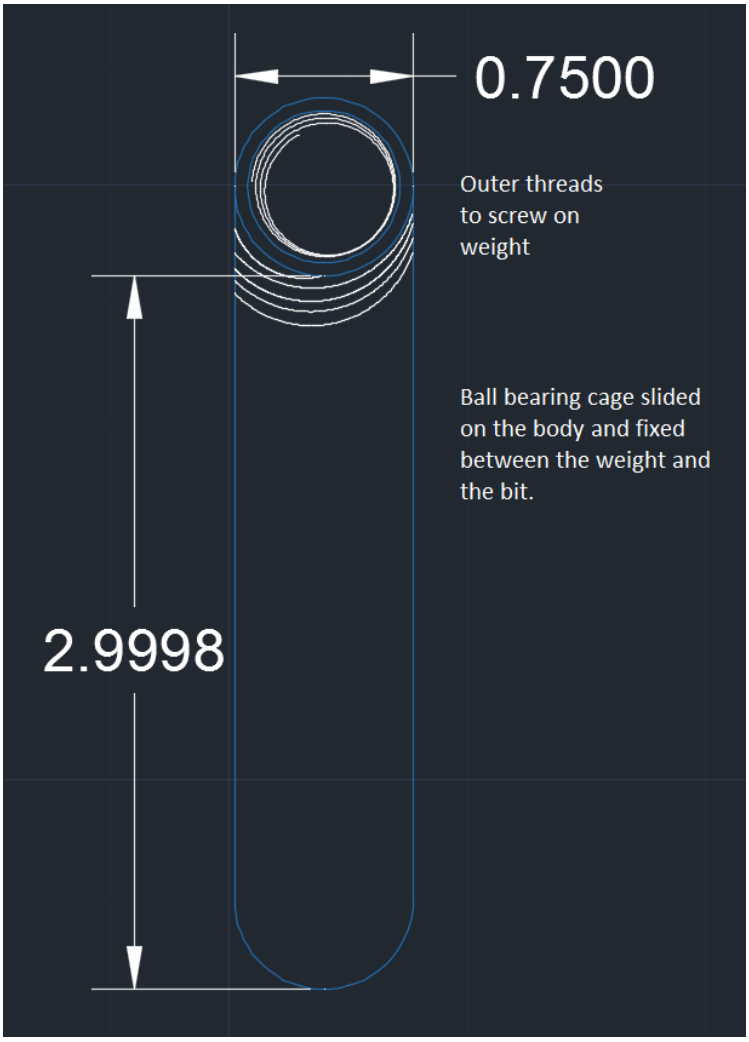

Fig. 17— Bit Sub

4.2 WOB using Bit Sub

In the previous year competition of Drillbotics 2015, the guidelines did not allow for us to attach anything on the drillstring other than sensors. Because of which the WOB was provided by the travelling block keeping the drillstring in compression. This compression caused bending and the magnitude of bending increased due to drillstring vibrations (i.e. whirl), increasing the chances of buckling due to bending. If the pipe is in tension the pipe can avoid any buckling altogether. Below proposed are the 2 methods for applying WOB using Bit Sub and keep the drillpipe in tension.

4.2.1 Attached Weight on Bit Sub

This year the guidelines allow us to attach weight on the bit sub up to 20 lbs which is the allowable WOB limit. The weight has been designed in such a way that it can be easily detached from the bit sub. The dimensions and design of the weight are described below. It is nothing but a regular hollow pipe with threads on one end on the inside. It is screwed on to the bit sub before the drillpipe is attached to the bit sub. The weight attached will act as a drill collar and provide the necessary WOB and keep the drillpipe in tension. Also the design of the weight will act as a casing or a borehole wall, restricting the drillpipe inside and preventing the pipe from excessive lateral displacement. If the weak drillstring was kept in compression then there would be bowing of the pipe which would be restricted by the casing and buckling due to excessive bending would have been prevented. But by keeping the drillpipe in tension the buckling of the pipe is avoided altogether. Also the weight is been stretched in length so that the centrifugal forces are less on the weight causing less lateral motion and vibration of the drillstring.

The weight is just a hollow steel pipe made of schedule 40 steel. The diameter of the hole drilled is 1.125 inch. Hence the 12 inches of the pipe has to be of outer diameter 1 inch and inner diameter 0.75 inch. The weight per foot for a schedule 40 pipe is given by **Eq. 30.**

$$W = 10.69 * (OD - t) * t = 10.69 * (1 - .125) * (0.125) = 1.169 \frac{lbs}{ft} \quad \text{..... (30)}$$

Hence 14.028 lbs gets accounted in the lower section of the weight which will travel inside the hole. The weight of the bit and sub is just over a pound. Rest 4.972 pounds of weight will be accounted by the extension of the same further up by 4.25 inch which makes the total length of the weight equal to 16.25 inch.

Testing and experiments will be carried out once the rig is ready to drill. The effect of the weight attached to the drillstring will be studied. If the drillstring vibrations are excessive due to the weight, then it will be unscrewed from the bit sub on competition day. Also in case the judges feel that the weight design stiffens the pipe, the weight will be removed. The following designed is proposed as a complimentary solution to keep the drillstring in tension.

4.2.2 Increasing Hydraulic Pressure

This method uses the principle of hydraulic pressure to apply WOB. By applying pressure across the constriction surface we create hydraulic force and a jet impact force on the bit and bit sub. A constriction will be placed inside bit sub before attaching it with the drill string. The constriction will be fixed on the latch and multiple constriction sizes will be created for different flowrates. Following is the constriction design, hydraulic calculations and the forces acting on the bit sub. The hydraulic force acting on the nozzle is given by **Eq. 31.**

$$F_{hyd} = A_c * \Delta P_b \quad \text{..... (31)}$$

$$F_j = 0.01823 * C_d * \sqrt{\rho_w * \Delta P_b} \quad \text{..... (32)}$$

$$\Delta P_b = \frac{8.311*10^{-5}*\rho*q^2}{C_d^2 A_t^2} \quad \text{..... (33)}$$

The weight of the bit is a little bit over a pound. Pressure drop across the bit using **Eq. 33** is equal to 76.84 psi for flowrate of 4.3 gpm. Hydraulic force on the bit using **Eq. 31** is 11.96 lbs. Jet impact force acting on the bit given by **Eq. 32** is equal to 1.88 lbs. The total forces acting on the bit is equal to 11.08 lbs in the downward direction acting as WOB. To have the drillpipe in tension additional 8.92 lbs of weight is needed. Using Eq.30 and Eq. 32 and a flow rate of 4.3 gpm, the diameter of the constriction needed is calculated as 0.167 inches. Using the above example, **Table 6** gives different constriction diameters with different flowrates.

Table 6— Calculations for Constriction Diameter

GPM	4.3	5	6
Pressure drop @ bit, psi	76.84	103.9	125.72
Hydraulic force, lbs	11.96	16.18	19.58
Jet impact force, lbs	1.88	2.19	2.4
Pounds needed, lbs	8.92	5.01	1.82
Dia. of constriction, in	0.167	0.19	0.23
Pressure drop across constriction, psi	60	24.6	7.4

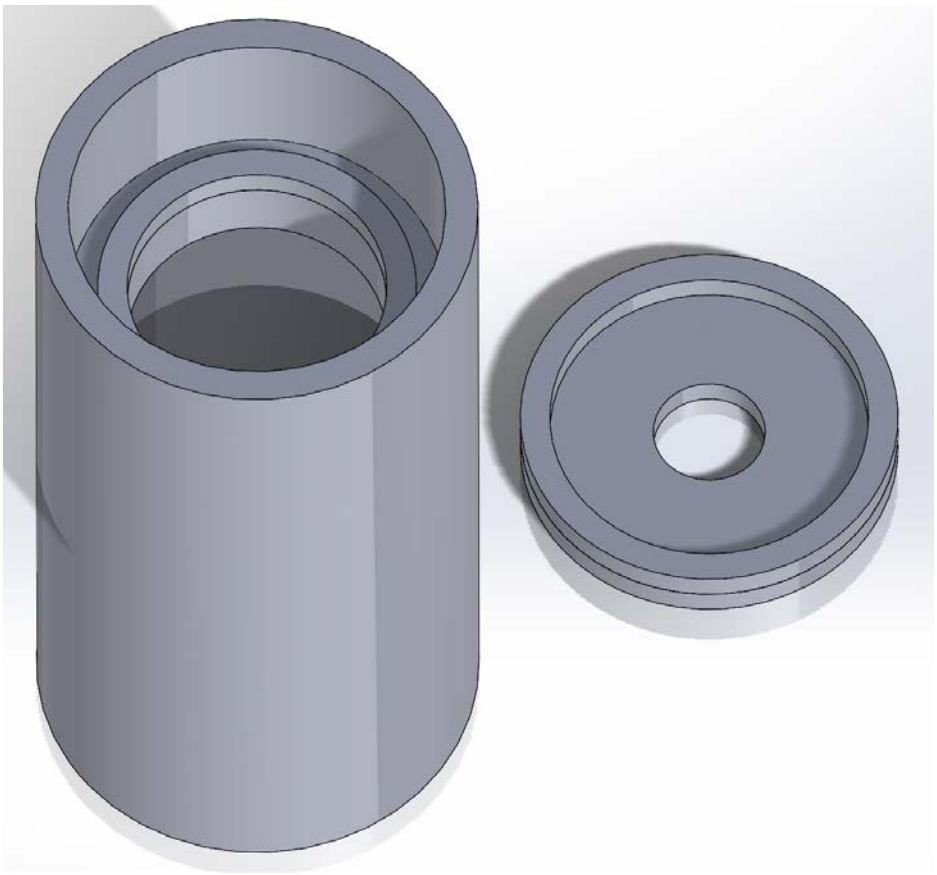

Fig. 18— Constriction Design

The constriction with different diameters will be prepared. It will be inverted and dropped inside the bit sub and will get fixed on the latch inside the bit sub.

5. Measurements, Sensors and Control System

5.1 Data Acquisition System

A data acquisition system is used to monitor the parameters measured by the sensors. It converts the change in current to a numerical value to provide to the control system. Depending on the value provided, the control system elects to take action or not. In the process of choosing a DAQ system, computer based control systems and programmable logic controllers were considered. The main parameters compared were the performance and the expense.

5.1.1 PC-Based Control

Devices communicate with a computer through an input/output card. Also, the computer based control system is not confined to one specific programing language, but supports a lot of them. Moreover, the

system is pretty good in terms of storing data and is cheap in comparison to the programmable logic controllers system. However, there are some downsides for the system such as the long booting time and locking up and crashing during operation.

5.1.2 Programmable Logic Controllers

Programmable logic controllers, PLC, monitor the inputs given to it continuously, to control the outputs based on the control program written. PLC system is robust which makes it a viable option in harsh environments. Also, the system is more reliable than the PC based control system. On the other hand, PLC depends on computers for human interface, management and data storing.

5.1.3 Control System

PC-Based control system was chosen for the design because it has the properties needed to automate the rig. For example, the system is flexible, cheap, and efficient in communicating between the control program and the rig. Also, the previous year's design used it and it proved efficient. The unit chosen to be used in the design is an Omega analog DAQ. The unit has four analog output channels and 16 analog input channels, as shown in the schematic in **Fig. 19**.

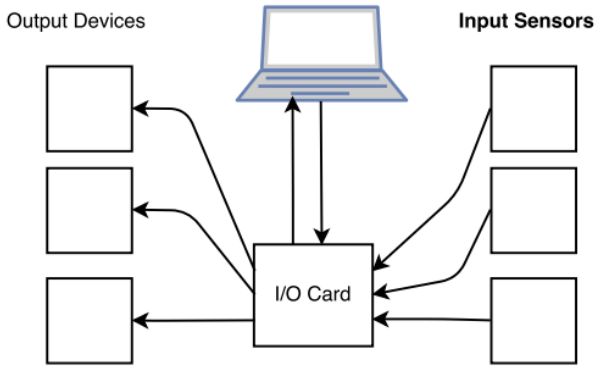

Fig. 19— Rough Schematic of the DAQ System

5.2 Measurements

In order to accomplish a better autonomous rig that needs no outside interference, the measurements of various parameters are monitored continuously. As a result, whenever a parameter is not in the range permitted by the system, action is taken to fix it. Some of the parameters that are monitored by the design are weight on bit (WOB), RPM and torque.

5.2.1 Pressure

Using pressure transducers, the pressure in the system will be regulated and monitored continuously through the whole drilling operation.

5.2.2 Current

Measuring the changes in the electrical supply, using a current measuring sensor, would assist in valuing the energy management in real time. Also, the mechanical specific energy could be estimated in real time, as well.

5.2.3 Weight on Bit (WOB)

To gain control over the WOB a load cell, shown in **Fig. 20**, is going to be used to assist the pneumatic cylinder. The sensor measures both compressional and tensional forces. The sensor will be place between the pneumatic cylinder piston's knuckle and the travelling block.

Fig. 20— Miniature Load Cell (After Omega 2015)

5.2.4 Torque and Rotational Speed (RPM)

Initially, an industrial bike torque sensor was considered due to its cheap price. However, from previous experience, they are not accurate or dependable. As a result, a more expensive option from Omega was chosen for its accuracy. The Omega sensor is a shaft to shaft torque sensor (**Fig. 21**). Also, to increases the accuracy of the reading, side force will be accounted for using load cells. The load cells, shown in **Fig. 22**, will be able to measure both compression and tension. Moreover, the torque sensor measures has an RPM sensor incorporated in it.

Fig. 21— Rotating Torque Sensor (After Omega 2015)

Fig. 22— Low Profile Load Cell (After Omega 2015)

5.2.5 Rate of Penetration (ROP)

Using an infrared displacement sensor, the depth of the bit will be measured. From this data the ROP would be measured.

5.2.6 Laser Distance Sensor

Laser distance sensor, shown below, is going to be used to assist in the vibration analysis. Also, by measuring the deviation of the drillstring, the deflection of the string could be minimized by changing other parameters such as ROP and WOB. Also, in the process of finding a fitting sensor, Inductive displacement sensor and capacitive displacement sensor were considered. However, the inductive sensor though is meant to study vibrations, it only works on conductive metals and the capacitive sensor has a range that is too small and accurate for the design.

Fig. 23— Laser Displacement Senor (After Automation Direct 2015)

5.2.7 Gyroscope and Accelerometer

Gyroscopes use earth's gravity and estimate the angular velocity they are undergoing. Using these data, a gyroscope could estimates the angles of deflection from the vertical axes to estimate its orientation. However, an accelerometer uses the G-force applied on it that is caused by acceleration. An accelerometer measuring at all three axes provides some information on the orientation, as well. As a result, using both the gyroscope and the accelerometer would provide a more accurate estimation. The sensors are meant to be mounted on the drillstring to minimize the deflection caused by the slanted formation. In order to find the right sensors, the range should be chosen for the application it is meant for. For example, if a gyroscope is meant to be used at 300 RPM, Using **Eq. 34** the needed range in degree/s is found to be approximately ±2000 deg/s.

$$\frac{Degree}{s} = RPM * \frac{360}{60} \quad \text{(34)}$$

5.3 Electrical Interference

Electrical interference was a large concern for the previous year's team and there was little done to prevent the problems that follow. Thus, for this competition, a grounding rod will be hammered into the earth and all high voltage equipment will be grounded to that rod. This is one step that will help alleviate electrical noise. Consideration for how electronics are wired and where VFD's are placed in respect to sensitive monitoring equipment will also decrease interference that is picked up by the sensors. Moreover, if needed, a magnetic shielding foil could be used to minimize the interference even further. These steps will in turn increase the ability of the rig to maintain optimum productivity.

5.4 Data Handling, Display and Cost

An updated VBA code of last year's algorithm will be used to handle the data input coming from multiple sensors. Also, the code will be able to store and process the data in real time. Using Excel, the data received from the sensors and their trends will be displayed on a computer screen. Some of the values the

code will be monitoring are WOB, depth, torque, ROP, orientation of drillstring, drillstring displacement, and pressure. The VBA program, will act as the control program of the rig. The control program will be interacting with both the rig equipment and the analog/digital sensors simultaneously and continuously during the drilling operation, to make the system efficient. The total Cost of sensors to automate the rig is show in **Table 7**. Table 6 only shows the cost of the main new equipment that was meant to improve last year's design.

Table 7— Automation Cost

Automation Cost			
Item	Vendor	Unit Cost, $	Quantity
Gyroscope/Accelerometer	CDI	23.16	1
Laser Displacmetn Sensor	Automation Direct	629	1
Load Cell	Omega	190	2
Load Cell	Omega	595	1
Torque/RPM sensor	Omega	1920	1
Contingency	-	354.716	10%
Total	-	3901.88	-

6. Cost Summary

The budget for the 2015-2016 Drillbotics competition is in the amount of $10,000 to improve upon the previous year's design. This budget will allow the team to purchase better monitoring equipment and afford the ability to build a redesigned rig structure. **Table 8** shows a summary of the materials to be purchased. Due to the team utilizing most of the previous year's components, the entire $10,000 allotment is not necessary. Contingency costs include the funds necessary to machine the bit sub, purchase fastening hardware and wiring materials. Although, as the season progresses in phase 2 of the design build, the extra funds may become helpful.

Table 8— Total Cost of the Design

Combined Build Cost		
Materials/Components	Cost (Including Previous Year Equipment), $	Cost (Excluding Previous Year Equipment), $
Aluminum Construction Materials	$745.00	$745.00
Linear Motion and Rotating Components	$1618.00	$1618.00
Sensors and Load Cells	$7055.35	$3901.88
Total	$9418.35	$6264.88

7. Conclusion

A detailed description of designing model drilling rig was provided in the report. The final design will be chosen based on economic, competition's guidelines, and safety factors. Information gained during the first phase of the competition will be verified in testing phase. Adjustments on the final design will be made if necessary.

Nomenclature

RPM	= Rotation per minute
WOB	= Weight on bit, lbf
q	= Flow rate, gpm
ρ_w	= Density of water, ppg
A_t	= Total cross-sectional area of bit nozzles/ constriction diameter, in^2
A_{act}	= Cross-sectional area, ft^2
C_d	= Discharge Coefficient
F_j	= Jet Impact Force, lbs
F_{hyd}	= Hydraulic Pressure Force, lbs
W	= Weight of foot, lbs/ft
OD	= Outer Diameter of the Weight, in
t	= Wall thickness of the weight, in
F_{hyd}	= Hydraulic force, lbs
A_c	= Total cross sectional area, in
ΔP_b	= Pressure drop across nozzle/ constriction
Ω_b	=backward non-slip whirl rate, cycles/s
Ω	=Whirl rate, cycles/s
F_s	=whirl rate ratio
V	=slip velocity, in/s
r_b	=radius of the borehole, in
r_{ds}	= radius of the drillstring, in
B	=Bending stress, psi
α	=phase angle, radian

t	=time, s
M	=bending moment, lb in
C	=distance from geometric center, in
A	=area of the drillstring, in^2
I	=moment of inertia, in^4
ρ	=radius of curvature, in
L	=original length, in
ΔL	=change in length, in
Θ	=angle of deflection
Fx_1	=swivel side force, lb
Fx_2	=stabilizer side force, lb
Fx_3	=bit side force, lb
ω_n	=natural frequency, cycle/s
k	=stiffness
m	=mass of the drillstring, lb
x	=displacement, in
ω	=frequency, cycle/s
EF	=excitation factor
b	= width of cut, in
dd	=diamond diameter, in
P	=total penetration, in
n_{eb}	=equivalent blade number
n_{bs}	= number of blades
ξ	=damping ratio, C/C_n

C_n =critical damping coefficient $C_n = 2\ I\ \omega_n$

C =damping coefficient

A_D = dimensionless whirl amplitude

Ω_D =dimensionless whirl rate, $\Omega_D = \frac{\Omega}{\Omega_n}$

T_{wlam} = shear stress at laminar flow

T_y = yield stress

K =consistency index

Re = Reynold's number

ρ =density

f =friction factor

U = fluid velocity, ft/s or m/s

Tw = frictional shear stress

P = pressure, psi

L = length, ft or m

D = diameter

C_d = discharge coefficient

References

Automation Direct. 2015. Laser Displacement Sensor, Automation Direct Inc., http://www.automationdirect.com/static/specs/perectoptcmos.pdf (Accessed November 2015)

Apostal, M.C., Haduch, G.A., et al. 1990. A Study to Determine the Effect of Damping on Finite-Element-Based, Forced Frequency-Response Models for Bottomhole Assembly Vibration Analysis. Presented at the 65th ATCE, New Orleans, LA, September 23-26. SPE-20458-MS. http://dx.doi.org/ SPE-20458-MS.

Bourgoyne, A.T., Millheim, K.K., Chenevert, M.E. et al. 1986. *Applied Drilling Engineering*, Vol. 2. Richardson, Texas: SPE Textbook Series.

Dodge, D.W. and Metzner, A.B. 1959. Turbulent Flow of non-Newtonian Systems. *AIChE Journal* **5** (2): 189-204.

Dykstra, M.W., Chen, D.C., et al. 1996.Drillstring Component Mass Imbalance: A Major Source of Downhole Vibrations. SPE Drilling and Completion **11** (4): 234-241. SPE-29350-PA. http://dx.doi.org/ SPE-29350-PA

Irvine, T. 1999. The Steady-State Response of a Single-Degree-of-Freedom-System Subjected to a Harmonic Force. *Vibrationdata.com*. Accessed October, 2015.

Jansen, J.D. 1992. Whirl and Chaotic Motion of Stabilized Drill Collars. *SPE Drilling Eng*. **07** (02): 107-114. SPE-20930-PA. http://dx.doi.org/ SPE-20930-PA.

Omega. 2015. Low Profile Load Cell. http://www.omega.com/googlebase/product.html?pn=LCHD-TP488&gclid=Cj0KEQiA4eqyBRDUh7Omv9vCtsoBEiQAspfs8uii8PNSVOycb_BHjHbtAwz8JgCcoOcdGrxYt1gh6t0aAv768P8HAQ (Accessed October 2015)

Omega. 2015. Miniature Load Cell. http://www.omega.com/pressure/pdf/LC203.pdf (Accessed December 2015).

Omega. 2015. Rotating Torque Sensor. http://www.omega.com/googlebase/product.html?pn=TQ513-200&gclid=Cj0KEQiAno60BRDt89rAh7qt-4wBEiQASes2tcbCnpZJ03t0fhloSUh6yD4Cgh7gLSG7I2X9HGwaBfYaAik78P8HAQ (Accessed November 2015).

Peterson, J.L. 1976. Diamond Drilling Model Verified in Field and Laboratory Tests. *JPT* **28** (02): 213-222. SPE-5072-PA. http://dx.doi.org/ SPE-5072-PA.

Vandiver, J.K., Nichoison, J.W., et al.1990. Case Studies of the Bending Vibration and Whirling motion of Drill Collars. Presented at SPE/IADC Drilling Conference, New Orleans, Louisiana, 28 February-3 March. SPE-18652-MS. http://dx.doi.org/ SPE-18652-MS.

Zhou, S., Yu, H., Hu, M. et al. 2012. Design of permanent magnet eddy current brake for a small scaled electromagnetic launch model. *J. Appl. Phys.* **111**(7): 07A738-1-07A738-3. http://dx.doi.org/10.1063/1.3679698.